



A Systems Biology-Based Computational Framework for Integrating Gut Microbiota-Derived Metabolites in Vascular Aging: The MCAS Model

Research Article

10.65520/erciyesfen.1871941

Imprint:

Volume: 42(1)

Year: 2026

Page: 191-206

- Erkan ÖZBAY^a
Serkan ÖRÜCÜ^b
Sami KARAGÖZ^c
Sait Ramazan GÜLBAY^d
Bülent IŞIK^e*

^a Lec. PhD., Karamanoğlu Mehmetbey University, erkanozbay@kmu.edu.tr

^b Asst. Prof., Karamanoğlu Mehmetbey University, srknorucu@kmu.edu.tr

^c Asst. Prof., Karamanoğlu Mehmetbey University, samikaragoz@kmu.edu.tr

^d MD, Karamanoğlu Mehmetbey University, ; saitramazan.gulbay@erbakan.edu.tr

^e Assoc. Prof., Karamanoğlu Mehmetbey University, bulentisik@kmu.edu.tr

* Corresponding Author

Received: 1/26/2026

Accepted: 3/18/2026

Citation:

Erkan ÖZBAY, Serkan ÖRÜCÜ, Sami KARAGÖZ, Sait Ramazan GÜLBAY & Bülent IŞIK, (2026). A Systems Biology-Based Computational Framework for Integrating Gut Microbiota-Derived Metabolites in Vascular Aging: The MCAS Model.

Erciyes University Journal of Institute Of Science and Technology, 42(1),

191-206

Hata! Yer işareti tanımlanmamış..

<https://doi.org/10.65520/erciyesfen.1871941>

Screened by



Except where otherwise noted, content in this article is licensed under a Creative Commons 4.0 International license. Icons by Font Awesome.

Abstract

Aging is a multifactorial process that is shaped by interconnected alterations in energy metabolism, epigenomic regulation, and chronic low-grade inflammation. Here, a multilayered computational model is described to integrate microbiome-derived metabolites with vascular aging-related biological features using a systems biology approach. A composite index that combines microbial, metabolic, and epigenomic components was constructed and analyzed based on publicly available datasets. An L2-regularized logistic regression model implemented with in a nested cross-validation scheme was employed to evaluate overall model behavior. The integrated model demonstrated consistently stable performance, with a mean AUC of 0.893 (95% CI: 0.787-0.959), a PR-AUC of 0.913, and a Brier score of 0.147. Ablation analyses further showed that microbial features contributed most strongly to model discrimination, while metabolic and epigenomic components mainly contributed to model stability. Taken together, this model provides an integrative computational approach for interpreting microbiota-associated biological patterns in relation to vascular aging.

Keywords: Gut microbiota, Vascular Aging, Systems Biology, Trimethylamine N-Oxide, Short-Chain Fatty Acids



Vasküler Yaşlanmada Bağırsak Mikrobiyotası Kaynaklı Metabolitlerin Entegrasyonu İçin Sistem Biyolojisi Temelli Hesaplamalı Bir Çerçeve: MCAS Modeli

Öz

Yaşlanma, enerji metabolizmasındaki, epigenomik düzenlemedeki ve kronik düşük dereceli inflamasyondaki birbiriyle bağlantılı değişiklikler tarafından şekillendirilen çok faktörlü bir süreçtir. Burada, mikrobiyom kaynaklı metabolitleri vasküler yaşlanma ile ilişkili biyolojik özelliklerle sistem biyolojisi yaklaşımını kullanarak bütünleştirmek için çok katmanlı bir hesaplamalı model tanımlanmaktadır. Mikrobiyal, metabolik ve epigenomik bileşenleri birleştiren bileşik bir indeks oluşturulmuş ve herkese açık veri kümelerine dayanarak analiz edilmiştir. İç içe geçmiş çapraz doğrulama şeması içinde uygulanan L2-düzenleştirilmiş bir lojistik regresyon modeli, genel model davranışını değerlendirmek için kullanılmıştır. Entegre model, ortalama AUC değeri 0.893 (95% GA: 0.787-0.959), PR-AUC değeri 0.913 ve Brier skoru 0.147 olmak üzere tutarlı biçimde kararlı bir performans göstermiştir. Ablasyon analizleri ayrıca mikrobiyal özelliklerin model ayırım gücüne en güçlü katkısı sağladığını, metabolik ve epigenomik bileşenlerin ise esas olarak model kararlılığına katkıda bulunduğunu göstermiştir. Tüm bunlar birlikte ele alındığında, bu model mikrobiyota ile ilişkili biyolojik örüntülerin vasküler

yaşlanma ile ilişkili olarak yorumlanması için bütünleştirici bir hesaplamalı yaklaşım sunmaktadır.

Anahtar kelimeler: Bağırsak Mikrobiyotası, Vasküler Yaşlanma, Sistem Biyolojisi, Trimetilamin N-Oksit, Kısa Zincirli Yağ Asitleri



1. Introduction

Aging is a multifaceted process that is commonly characterized by progressive alterations in bioenergetic pathways, gradual epigenomic remodeling, and persistent low-grade inflammatory signaling [1, 2]. Over time, these interconnected mechanisms influence tissue homeostasis and progressively reshape the biological characteristics of senescence. Among organ systems, the circulatory network appears particularly sensitive to systemic perturbations, where sustained hemodynamic load and chronic inflammatory cues are thought to contribute to reduced vascular compliance, diminished nitric oxide bioavailability, and increased arterial stiffness. At the same time, vascular aging retains a degree of biological plasticity, particularly in relation to regulatory and metabolic adaptation, suggesting that its progression may not be fully explained by hemodynamic factors alone [3-5]. Recent evidence further suggests that systemic biological regulators, including host-microbiota interactions and microbiota-derived metabolites, may contribute to vascular aging-associated molecular processes.

Against this biological backdrop, the gut microbiome is increasingly recognized as an active regulatory ecosystem rather than a passive microbial reservoir [6]. Age-associated shifts in microbial composition, including changes in the *Firmicutes-Bacteroidetes* ratio, have been described across multiple studies. Although these alterations often appear modest at the compositional level, reductions in butyrate-producing taxa have been associated with patterns of enhanced proinflammatory molecular activity [7-11]. Such compositional shifts are not limited to taxonomic variation but are also accompanied by measurable changes in microbial metabolic output. Alterations in microbial community structure directly influence the spectrum of metabolites released into the host circulation, thereby linking microbial population dynamics with host molecular signaling processes. Concurrently, such microbial reorganization has also been linked to decreased short-chain fatty acid (SCFA) production and increased levels of trimethylamine N-oxide (TMAO) [8,10,12-16]. These metabolite fluctuations represent a functional interface through which microbial activity can influence vascular physiology and inflammatory signaling within the host. Taken together, these coordinated changes support the view that microbial metabolism may play a modulatory role in shaping epigenomic regulation and vascular-associated biological processes.

Specific microbiota-derived metabolites have been linked to distinct molecular pathways relevant to vascular aging and increasingly appear to function as biologically active signaling molecules capable of influencing host vascular gene expression patterns. Rather than acting solely as metabolic by-products, metabolites such as short-chain fatty acids (including butyrate) and trimethylamine N-oxide (TMAO) participate in molecular signaling processes that modulate transcriptional regulation, inflammatory responses, and endothelial cellular behavior [13,17,18]. Through these signaling processes, microbial metabolites serve as molecular intermediaries that translate microbial activity into host cellular responses, including modifications in transcriptional activity and chromatin-associated regulation. TMAO has been reported to be associated with activation of the ROS-TXNIP-NLRP3 signaling cascade, a pathway that has been shown to contribute to endothelial dysfunction and cellular senescence. In contrast, phenylacetic acid (PAA) has been connected to accelerated endothelial deterioration, whereas butyrate is generally considered to exert protective effects, in part through histone deacetylase (HDAC) inhibition [16,17,19-21]. These mechanisms illustrate how metabolite signaling can propagate from microbial metabolic activity to intracellular regulatory pathways that influence vascular cellular behavior. Epigenomic regulatory mechanisms (including processes such as histone acetylation, methylation, and noncoding RNA-mediated modulation) play central roles in shaping vascular gene expression patterns during aging. Within lipid metabolism, the ABCA1-miR-27a/b axis has also been implicated in cholesterol handling

and the maintenance of vascular elasticity [14,22]. Overall, these observations indicate that microbiota-derived metabolites exert condition-specific biological effects rather than acting as uniformly beneficial or deleterious agents.

Whether aging can be attributed primarily to microbial imbalance or instead reflects a broader adaptive interplay between host biology and time remains unresolved. Analyses focused solely on microbial composition tend to capture only a limited portion of this complexity, as metabolic dynamics and epigenomic responses are tightly interconnected. Microbial composition determines the repertoire of metabolites produced within the gut ecosystem, while these metabolites can subsequently influence host regulatory pathways through signaling processes that affect gene expression and cellular behavior. Consequently, microbial population structure, metabolite production, and epigenomic regulation represent sequentially interacting biological layers rather than independent analytical domains. Addressing this multidimensional structure therefore requires integrative approaches capable of jointly representing microbial, metabolic, and epigenomic layers [23]. Data-driven systems biology and computational modeling provide a structured approach for such integration [23, 24].

Although numerous studies have examined associations between gut microbiota composition and aging-related phenotypes, several methodological limitations remain. A substantial proportion of existing analyses rely primarily on taxonomic profiling or other single-layer analytical strategies centered on microbial composition. While these approaches have provided important descriptive insights, microbial composition alone may not sufficiently represent downstream metabolic activity or the regulatory processes through which microbial signals influence host physiology. In particular, microbiota-derived metabolites participate in molecular pathways that can affect transcriptional regulation, inflammatory signaling, and cellular homeostasis. Evaluations restricted to compositional variation may therefore capture only a limited portion of the biological processes associated with vascular aging. Recent developments in systems biology indicate that age-associated phenotypes are shaped by coordinated interactions among microbial communities, metabolite-related activity, and host regulatory mechanisms [23,25]. Analytical strategies capable of jointly representing these interacting biological layers may therefore provide a more comprehensive interpretation of microbiota-associated patterns observed during vascular aging. In this context, the Microbial Cardiovascular Aging Signature (*MCAS*) model integrates microbial composition, metabolite-associated indicators, and epigenomic surrogate variables within a unified analytical structure designed to examine vascular aging-related biological variation.

The *MCAS* model was conceptually developed based on systems biology principles, microbiome-derived metabolite signaling models, and composite aging signature methodologies [1,23,26,27]. *MCAS* integrates three interrelated dimensions: microbial composition (M), metabolite-associated dynamics (K), and epigenomic indicators (E). In this formulation, $M(t)$ represents microbial aging-related features, $K(t)$ captures metabolite-associated variation, and $E(t)$ reflects epigenomic regulatory responses. The composite outcome variable, $V(t)$, is intended to analytically represent vascular aging-related biological characteristics, including arterial stiffness and endothelial alteration [28,29]. Given the broad biological relevance of vascular aging processes, application of integrative models such as *MCAS* provides a structured approach for examining multi-layer biological interactions in population-level datasets [30].

The *MCAS* model was developed to address methodological limitations observed in current microbiome-based aging studies by linking microbial composition, metabolite-associated activity, and host regulatory responses within a single analytical representation. In this approach, microbial community structure can be considered an upstream biological layer that influences the spectrum of metabolites produced within the gut ecosystem. These metabolites may subsequently act as signaling intermediaries capable of modulating vascular cellular processes through inflammatory signaling pathways, transcriptional regulation, and chromatin-associated modifications. Epigenomic responses can therefore reflect downstream regulatory processes through which metabolite-associated signals may influence vascular gene expression patterns and endothelial cellular behavior. By analytically relating these sequential biological layers, the *MCAS* model allows microbial population dynamics,

metabolite-associated signaling, and regulatory responses to be examined together rather than as independent analytical variables. This integrative analytical strategy may support a more comprehensive interpretation of microbiota-associated biological variation beyond taxonomic profiling alone and may facilitate the investigation of how microbial metabolic activity and host regulatory processes could jointly relate to vascular aging-associated biological patterns.

2. Materials and Methods

This study utilized anonymized, publicly available human microbiome datasets reported by Yatsunenko et al. (2012) [7]. The datasets were obtained from the MG-RAST server using the accession identifiers qiime:850 for 16S rRNA sequencing data and qiime:621 for shotgun metagenomic data, from which raw sequencing datasets were downloaded and subsequently processed within the analytical pipeline developed in the present study (Figure 1).

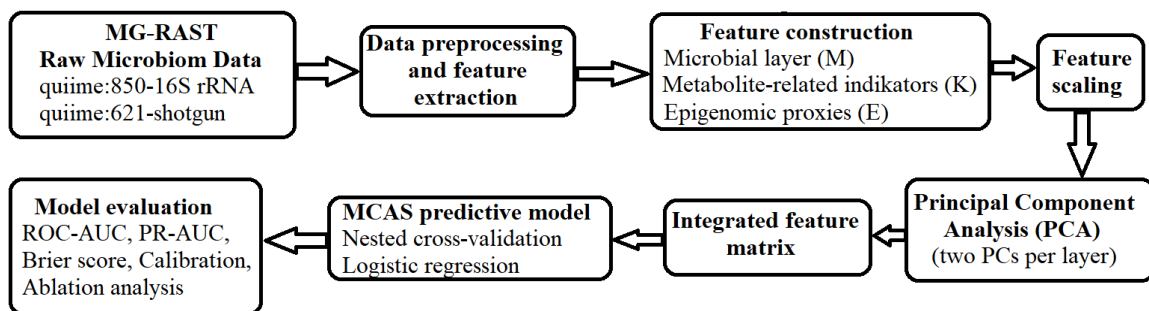


Figure 1. Analytical pipeline of the *MCAS* model. Raw microbiome sequencing datasets were obtained from the MG-RAST repository (accessions qiime:850 and qiime:621). Microbial composition features were used to construct the microbial layer (*M*), while metabolite-associated indicators (*K*) and epigenomic surrogate indicators (*E*) were derived from literature-informed biological associations. Each layer was standardized and subjected to principal component analysis (PCA), and the first two components per layer were integrated into a feature matrix used for the *MCAS* predictive model based on L2-regularized logistic regression evaluated using nested cross-validation (outer folds = 5, inner folds = 3). Model performance was assessed using ROC-AUC, PR-AUC, and Brier score metrics

2.1. Data Source and Preprocessing

All analyses were performed using Python 3.10 and relied on publicly available microbiome datasets obtained from open-access repositories (MG-RAST; MG-RAST accessions qiime:850 for 16S rRNA sequencing and qiime:621 for shotgun metagenomic data) [7]. The analytical structure was organized into three analytical modules. At the microbial layer (*M*), taxonomic profiles and age-associated pathway characteristics were examined. The metabolic layer (*K*) focused on indices associated with microbiota-derived metabolites frequently linked to vascular physiology, including short-chain fatty acids (SCFAs), trimethylamine-N-oxide (TMAO), and phenylacetic acid (PAA). The epigenomic layer (*E*) incorporated literature-informed surrogate indicators derived from known biological associations between these metabolites and host regulatory processes. Specifically, this layer represented pathways associated with SCFA-related histone deacetylase (HDAC) inhibition and Nuclear Factor kappa B (NF- κ B)-associated transcriptional and chromatin-related regulatory signals linked to TMAO and PAA.

Each module was normalized independently within the training partitions of the nested cross-validation procedure. Dimensionality reduction was then carried out using principal component analysis (PCA), from which the first two principal components were retained per module (meta_PC1/2, metabo_PC1/2, epi_PC1/2), resulting in a total of six integrated features. The first two principal components were retained because they capture the dominant variance structure of the feature space while maintaining a compact representation suitable for predictive modeling. The aggregated feature matrix is reported in sheet *integrated_matrix* of *S8-integrated_matrix and labels* file. To prevent data leakage and ensure reproducibility, PCA fitting was limited to training subsets and subsequently

applied to the corresponding test data. Detailed preprocessing workflows, directory structures, and execution pipelines are described in the *S1-Supplementary Notes*, and all analysis scripts are provided in *S6-Code Description*.

To improve the transparency and navigability of the supplementary datasets, a structured Data Dictionary defining all analytical variables used in the integrated matrix and model inputs is provided in *S2-Data Dictionary*. In addition, a summarized representation of the biological content of the microbial (M), metabolic (K), and epigenomic (E) modules is presented in *Supplementary Table S13 (Table_S13)* to facilitate interpretation of the module-specific analytical variables used in the MCAS model.

2.2. Formulation of MCAS Model

The MCAS model was formulated as follows:

$$V(t) = \alpha M(t) + \beta K(t) + \gamma E(t) + \delta [M(t) \cdot K(t) \cdot E(t)] \quad (1)$$

In this formulation, $V(t)$ represents a vascular aging-related composite index. The coefficients of the predictive model were estimated during the nested cross-validation training procedure using logistic regression. The coefficients α , β , and γ denote empirically derived weights assigned to each layer, while δ represents a conceptual interaction component describing the joint contribution of the three biological layers and is not estimated as a parameter in the predictive model. Equation (1) therefore represents a conceptual formulation of the MCAS model rather than the explicit mathematical structure used in the predictive analysis. This interaction component is not implemented as an explicit interaction term within the logistic regression model used in the predictive analysis.

The microbial layer $M(t)$ includes features related to microbial community composition and pathway-level microbial activity. The metabolic layer $K(t)$ reflects metabolite-associated variation derived from the processed feature space. The epigenomic layer $E(t)$ encodes surrogate indicators of transcriptional regulatory responses influenced by microbial metabolites. In the predictive modeling workflow, these biological layers are represented by principal component-derived features (meta_PC1/2, metabo_PC1/2, epi_PC1/2) obtained during the preprocessing stage.

2.3. Machine Learning and Evaluation

Model training and validation were carried out using a nested cross-validation design, consisting of five outer folds and three inner folds. Feature standardization and PCA fitting were applied solely within the training folds, and the resulting transformation parameters were then applied to the corresponding test data to prevent data leakage. Classification was performed using an L2-regularized logistic regression model with class-weight balancing to account for class imbalance [24]. Logistic regression was selected as the primary classifier because its relatively low model complexity reduces overfitting risk and improves interpretability in datasets with limited sample sizes and biologically structured feature sets.

Model performance was evaluated using three complementary metrics: the area under the receiver operating characteristic curve (AUC), the precision-recall area under the curve (PR-AUC), and the Brier score. Ninety-five percent confidence intervals for AUC estimates were obtained through non-parametric bootstrapping with 500 resampling iterations [31]. Detailed data-processing workflows, validation procedures, and executable scripts are provided in *S1-Supplementary Notes* and *S6-Code Description*. Given the relatively limited sample size, the nested cross-validation design combined with bootstrap confidence interval estimation was used to provide a conservative and robust assessment of model performance.

2.4. Predictive Modeling and Ablation Analyses

Classification analyses were conducted using the same L2-regularized logistic regression model within the nested cross-validation design described above.

Ablation analyses were performed in order to examine the relative contribution of each feature layer. Seven model configurations were evaluated, including microbial-only (M), metabolic-only (K), epigenomic-only (E), pairwise combinations ($M+K$, $M+E$, $K+E$), and the fully integrated model ($M+K+E$). Comparative assessments were primarily based on AUC values to evaluate differences in discriminative performance among configurations. Machine-readable summaries of all evaluation results are provided in *S4-Model Metrics* and *S5-Ablation Results*.

2.5. Network Representation

Tables summarizing the literature-supported associations used to construct the network representation are provided in *Supplementary Table S12 (Table_S12)* and *Supplementary Table S13 (Table_S13)*. The network representation depicts literature-supported associations between gut microbiota-derived metabolites, including SCFAs, TMAO, and PAA, and biological processes related to vascular aging, such as endothelial dysfunction, oxidative stress (OS), arterial stiffness, and myocardial remodeling. This network is intended as a descriptive conceptual summary rather than an empirically inferred interaction map, and serves to synthesize biological relationships that have been previously reported in the literature [26].

2.6. Ethical Approval

This study received approval from the Karamanoğlu Mehmetbey University Medicine Faculty Scientific Ethics Committee (date: 09 December 2025; approval no: 26-2025/23). The study was conducted in accordance with applicable ethical standards and the principles of the Declaration of Helsinki. As the analyses were based solely on previously collected, anonymized, and publicly available datasets, no direct participant involvement occurred and informed consent was therefore not required.

3. Results

3.1. Features Extracted via Principal Component Analysis (PCA)

The processed dataset contained two PCA-derived components (meta_PC1/2, metabo_PC1/2, epi_PC1/2) for each analytical module-microbial, metabolic, and epigenomic. These six components were subsequently combined to form an integrated feature matrix used for downstream analyses. A summary of the variables included in each module and their biological interpretation is provided in *Supplementary Table S13 (Table_S13)*, while complete variable definitions are documented in the *S2-Data Dictionary*.

3.2. Receiver Operating Characteristic (ROC), Precision-Recall Area Under the Curve (PR-AUC), and Calibration Analyses

In the fully integrated *MCAS* configuration ($M+K+E$), the mean ROC-AUC was calculated as 0.893 (95% CI: 0.787-0.959), with a corresponding PR-AUC of 0.913 and a Brier score of 0.147. The receiver operating characteristic (ROC) curve is illustrated in *S7-Figures and Supplementary Figures (Supplementary Figure S1)*. Calibration analyses comparing predicted and observed outcome probabilities are illustrated in *S7-Figures and Supplementary Figures (Supplementary Figure S2)* and summarized in *S4-Model Metrics*. External validation across independent populations was not undertaken in this study.

3.3. Ablation Analyses

The contribution of individual *MCAS* components was examined through ablation analyses [23,27,32]. The microbial-only configuration (M) yielded an AUC of 0.847, whereas the metabolic-only (K) and epigenomic-only (E) configurations produced AUC values of 0.640 and 0.570, respectively. For paired combinations, the $M+K$ model achieved an AUC of 0.893, the $M+E$ model reached 0.842, and the $K+E$ model resulted in an AUC of 0.656. A graphical comparison of model configurations is presented in *S7-Figures and Supplementary Figures (Supplementary Figure S3)*.

The fully integrated $M+K+E$ configuration produced an AUC value (0.893) identical to the $M+K$ model. Complete ablation results for all model configurations are provided in *S5-Ablation Results*.

3.4. Schematic Network and Biological Interpretation

SCFAs have been associated with endothelial stability, whereas TMAO and PAA have been linked to inflammatory processes and age-related cellular deterioration. These associations reflect relationships previously reported in the literature rather than representing novel empirical findings [9,12,13,21,26,33]. The network representation summarizes literature-supported interactions between microbiome composition, metabolite-associated signals, and epigenomic regulatory features included in the *MCAS* model.

4. Discussion and Conclusion

In this study, the *MCAS* model is best interpreted as a biologically informed vascular aging signature derived from microbial, metabolic, and epigenomic analyses, rather than as a standalone predictive algorithm. The analytical approach was designed to combine microbial, metabolic, and epigenomic features within a systems biology perspective, without implying direct clinical prediction or diagnostic utility.

Across the analysis, patterns suggesting potential coordinated relationships between epigenomic regulatory signals and SCFA-related metabolic activity were identified in relation to vascular aging processes. Previous experimental and observational studies report that butyrate is associated with vascular stability. The reported mechanisms include endothelial nitric oxide synthase (eNOS) activity, mitochondrial biogenesis, and HDAC inhibition [8,16,17,20]. In parallel, epigenomic processes such as histone acetylation, methylation, and non-coding RNA-mediated regulation have been described as modulators of SCFA-related responses, whereas pro-inflammatory signals associated with TMAO and PAA have been connected to transcriptional alterations in vascular tissues. Associations between TMAO, PAA, ROS generation, NF- κ B activation, and broader epigenomic processes indicate that these effects may depend on biological conditions and metabolite concentration [21]. Accordingly, prior studies have emphasized that the systemic biological effects of SCFAs, TMAO, and PAA vary substantially and should be interpreted cautiously, particularly in therapeutic or translational settings [18,19]. Comparable observations have also been reported in multi-omic investigations across different analytical platforms [15,25,34].

In the ablation analyses, the addition of the epigenomic module did not produce an increase in discriminative performance compared with the $M+K$ configuration. However, the integrated model showed acceptable calibration characteristics and a relatively low Brier score, indicating stable predicted probability estimates. These observations suggest that the epigenomic layer may primarily contribute to capturing regulatory signals associated with microbial metabolite activity rather than to improving classification performance. Although a two-layer ($M+K$) configuration may be sufficient for discrimination in this dataset, the inclusion of the E module may be justified when the objective includes probability calibration and biological interpretability.

Within the *MCAS* model, epigenomic surrogate indicators $E(t)$ are used to represent regulatory responses associated with microbial metabolite signals. SCFA-associated features were linked to mechanisms such as HDAC inhibition and increased histone acetylation [9, 34], whereas inflammatory cascades linked to TMAO and PAA have been associated with NF- κ B activation, inflammasome signaling, and cellular senescence markers [13,15,21,35]. These observations suggest that microbiota-related influences extend beyond metabolic variation and are also reflected in epigenomic regulatory layers. Future experimental validation using high-resolution approaches, such as single-cell epigenomic profiling or targeted perturbation strategies, would be required to further clarify these relationships.

In the analyzed dataset, the *MCAS* model demonstrated stable discriminative performance broadly comparable to previously reported microbiome-based aging models [1,27]. The integrated representation of microbial [$M(t)$], metabolic [$K(t)$], and epigenomic [$E(t)$] components may contribute

to this performance, while the *MCAS* predictive model showed consistent performance across validation folds. However, the absence of external validation limits the generalizability of these findings. In addition, net reclassification improvement (NRI) and integrated discrimination improvement (IDI) analyses were not performed in the present study, and future studies should evaluate whether such models capture biological aging signals beyond chronological age [36,37].

The *MCAS* model integrates microbial, metabolic, and epigenomic information to capture vascular aging-related biological patterns. Unlike taxonomy-focused microbiome clocks [1], it adopts a multi-layer analytical model that is conceptually related to approaches used in multi-view learning and multi-omic data integration [27]. In this respect, *MCAS* is aligned with emerging multi-omic modeling strategies that emphasize integrated analysis of heterogeneous biological data rather than reliance on single-domain predictors [25].

From a translational perspective, the *MCAS* model highlights epigenomic and metabolite-related mechanisms that have been discussed in prior literature as potential modulators of vascular aging, including SCFA-associated regulation and pathways linked to TMAO and PAA [38-40]. Nevertheless, any therapeutic or prognostic implications remain speculative and require careful evaluation, given that the biological effects of these metabolites can vary depending on physiological and environmental conditions [18,19,41]. Earlier studies describing microbiota-based modulation of SCFA and TMAO profiles further illustrate both the potential and the complexity of such approaches [8,16,29,42].

Several limitations of this study should be acknowledged. The analyses were based on publicly available, cross-sectional microbiome datasets [7], which restrict the ability to assess temporal dynamics of vascular aging. Metabolomic and epigenomic features were represented using surrogate indicators rather than direct molecular profiling [7, 43]. Additionally, the relatively modest cohort size may have constrained the statistical stability and generalizability of the model. Although precautions were taken to minimize data leakage during model preprocessing and validation procedures, some residual overfitting may still be present. Information on dietary patterns, medication use, and comorbid conditions was only partially available, and therefore causal interpretations should be avoided.

Future studies incorporating longitudinal designs, direct multi-omic measurements, and validation across diverse populations will be essential for further evaluation of the robustness and applicability of the *MCAS* model. *MCAS* should therefore be interpreted as an integrative analytical approach rather than a clinical decision-making tool. From a clinical standpoint, it is not intended to replace established cardiovascular risk assessment models but may complement them by capturing microbiota-associated metabolic signals and epigenomic proxy indicators related to vascular aging that are not reflected in conventional clinical parameters.

Data Availability

This study is based on the re-analysis of publicly available datasets. The microbiome data analyzed in this work were obtained from the study by Yatsunenکو et al. (2012) [7]. No new raw sequencing, metabolomic, or epigenomic data were generated as part of this analysis.

Processed data matrices, model predictions, summary performance metrics, and ablation analysis results used for training and validation are provided in *S8-integrated_matrix and labels*, *S3-Dataset Description*, *S4-Model Metrics* and *S5-Ablation Results*, along with the corresponding *S9-Source_Data*, analysis scripts, documentation, and reproducibility resources. *S3-Dataset Description* describes dataset provenance and the structure of the processed *MCAS* input matrices. The associated MG-RAST accession identifiers are qiime:850 for 16S rRNA sequencing data and qiime:621 for shotgun metagenomic data. For transparency, the original public datasets corresponding to Tables S1-S12 are also included in the supplementary materials without modification. Detailed information regarding file organization and reproducibility procedures is provided in the *S1-Supplementary Notes*. A detailed Data Dictionary describing all analytical variables and module assignments is provided as *S2-Data Dictionary* to define the variables used in the processed analytical datasets.

Code Availability

Static versions of all scripts used for model construction and analytical evaluation, and figure generation are provided in *S6-Code Description* and in the primary analysis script (*MCAS_scripts*). These materials are intended to enable reproduction of all reported analyses. All software dependencies, version information, and data file paths are explicitly documented.

Each stage of the analytical workflow, including feature preprocessing and the nested cross-validation strategy, is described in detail in the *S1-Supplementary Notes*.

Supplementary Materials

Supplementary Information accompanying this article has been reorganized to improve clarity and navigability of the supporting datasets. The supplementary materials are structured into modular components that separately document processed data matrices, variable definitions, analytical outputs, and reproducibility resources.

S8-integrated_matrix and labels contains the integrated feature matrix used for model training, including the six principal components derived from the microbial (*M*), metabolic (*K*), and epigenomic (*E*) analytical modules, together with the corresponding sample identifiers. The machine-readable class labels used for supervised model training are provided separately in sheet *labels* of *S8-integrated_matrix and labels* file. *S3-Dataset Description* describes the origin and structure of the processed datasets used in the analysis.

To ensure that readers can easily interpret all variables used in the analyses, a comprehensive Data Dictionary is provided as *S2-Data Dictionary*. This document defines each variable included in the analytical datasets, specifies its module membership (*M*, *K*, or *E*), describes its biological interpretation, and identifies its source within the preprocessing pipeline.

In addition, datasets and analytical descriptions of the biological variables are provided in *Supplementary Tables S1-S13*. These tables include publicly available dataset summaries and analytical descriptions related to the variables used in the *MCAS* model. In particular, *Supplementary Table S13* provides a concise overview of the microbial (*M*), metabolic (*K*), and epigenomic (*E*) modules, including their biological interpretation and analytical roles within the *MCAS* model.

S4-Model Metrics and *S5-Ablation Results* provide machine-readable summaries of model evaluation metrics and ablation analyses in JSON format. *S9-Source_Data* files contain numerical values underlying the ROC, PR-AUC, calibration, and ablation figures reported in the main text.

S6-Code Description materials include *MCAS_scripts.txt* and *S6-Code Description* which contain all scripts used for model construction and analytical evaluation, model training, validation, and figure generation. The analytical workflow, including preprocessing steps, feature preprocessing procedures, model parameters, and directory organization required for reproducing the analyses, is described in detail in the *S1-Supplementary Notes*.

Structure of the Supplementary Materials

To facilitate transparency and reproducibility, the supplementary materials accompanying this article are organized into the following structured components.

Supplementary Documentation

S1-Supplementary Notes: Detailed description of preprocessing steps, dimensionality reduction procedures, model parameters, directory structure, and reproducibility instructions.

S2-Data Dictionary: Comprehensive definition of all analytical variables used in the integrated datasets, including module assignments and biological interpretation.

Supplementary Data

S3-Dataset Description

Dataset Provenance and Structure: Documentation describing the origin of the processed datasets, including MG-RAST accession identifiers, dataset structure, and preprocessing context.

S4-Model Metrics

Model Performance Metrics: Machine-readable JSON file summarizing nested cross-validation results for the MCAS model, including mean AUC, PR-AUC, Brier score, and bootstrap-derived confidence intervals.

S5-Ablation Results

Ablation Analysis Results: Machine-readable JSON dataset reporting performance metrics for all evaluated model configurations (M , K , E , $M+K$, $M+E$, $K+E$, and $M+K+E$).

S8-integrated_matrix and labels

Integrated Feature Matrix (sheet integrated_matrix of S8-integrated_matrix and labels file): Processed feature matrix used for model training. The dataset contains six PCA-derived components representing the microbial (M), metabolic (K), and epigenomic (E) modules (meta_PC1, meta_PC2, metabo_PC1, metabo_PC2, epi_PC1, epi_PC2) together with corresponding SampleID values.

Sample-Level Class Labels (sheet labels of S8-integrated_matrix and labels file): Machine-readable dataset containing binary class labels used in model training (Class: 0 = healthy/younger, 1 = vascular-aged).

Supplementary Tables

Table S1-S11: These tables correspond to publicly available datasets originally reported by Yatsunenko et al. (2012) and are provided here unchanged to facilitate reader access to the underlying microbiome resources. They represent original publicly available microbiome datasets and are included for reference without modification.

Table S12 - Network Representation Data: Structured dataset supporting the schematic network representation linking microbiota-derived metabolites with vascular aging-related biological processes.

Table S13 - MCAS Module Definitions: Overview of the microbial (M), metabolic (K), and epigenomic (E) modules used in the MCAS model, including variable definitions, biological interpretation, and analytical roles within the model.

Supplementary Figures

S7-Figures and Supplementary Figures

Figure S1 - Receiver Operating Characteristic (ROC) Curves: ROC curves generated from outer-fold predictions in the nested cross-validation procedure.

Figure S2 - Calibration Analysis: Calibration plot comparing predicted and observed outcome probabilities, accompanied by predicted probability distribution.

Figure S3 - Ablation Analysis Comparison: Graphical comparison of model performance across all evaluated MCAS model configurations.

Supplementary Code

S6-Code Description

MCAS_scripts.txt: Primary analysis script implementing preprocessing, nested cross-validation, model training, evaluation metrics, calibration analysis, and ablation experiments.

Supplementary Code_MCAS: Executable supplementary code used to reproduce the analytical workflow described in the manuscript.

Source Data

S9-Source_Data contains the numerical values underlying the figures reported in the manuscript, including ROC curves, calibration analyses, and ablation performance metrics.

Supplementary Materials Checklist

To enhance transparency and reproducibility, the supplementary materials were prepared according to widely adopted data and code availability standards commonly used by major scientific publishers.

Data Availability

- ✓ Public datasets used in the study are clearly identified (Yatsunenکو et al., 2012 [7]; MG-RAST accessions qiime:850 and qiime:621).
- ✓ Processed analytical datasets used for model development and validation are provided.
- ✓ All datasets used in the analyses are included within *S3-Data Description*, *S4-Model Metrics*, *S5-Ablation Results*, *S8-integrated_matrix and label* files.
- ✓ Source Data underlying the reported figures are available (*S9-Source_Data*).

Code Availability

- ✓ All scripts used for model construction and analytical evaluation, model training, validation, and figure generation are provided.
- ✓ Code file (*S6-Code Description*) include *MCAS_scripts* and *Supplementary_Code_MCAS*.
- ✓ Software environment and computational dependencies are documented (Python 3.10).
- ✓ The analytical workflow is described in detail in the *S1-Supplementary Notes*.

Reproducibility

- ✓ Data preprocessing workflow is documented.
- ✓ Procedures used for generating the analytical variables are documented.
- ✓ Nested cross-validation design is specified (outer folds = 5; inner folds = 3).
- ✓ Hyperparameter tuning procedures are documented.
- ✓ Evaluation metrics are reported (ROC-AUC, PR-AUC, and Brier score).
- ✓ Bootstrap-based confidence interval estimation is described.

Supplementary Files

- ✓ All supplementary files referenced in the main text are provided.
- ✓ File numbering follows a consistent format (*S3-Data Description*, *S4-Model Metrics*, *S5-Ablation Results*, *S8-integrated_matrix and label*, *Tables S1-S13*, *S7-Figures and Supplementary Figures*).
- ✓ Machine-readable datasets are included (CSV and JSON formats).

- ✓ Variable definitions and metadata are documented in the *S2-Data Dictionary*.

Figures and Numerical Data

- ✓ Numerical values underlying the figures are provided as *S9-Source_Data* file.
- ✓ ROC, calibration, and ablation outputs are reproducible using the provided scripts.
- ✓ Machine-readable summaries of model evaluation results are provided in JSON format.

Transparency and Documentation

- ✓ Dataset provenance is documented.
- ✓ The analytical pipeline is described in detail.
- ✓ Variable definitions are provided.
- ✓ Biological interpretation of model modules is documented.



Peer-review: External, Independent.

Acknowledgements:

-

Declarations:

1. Statement of Originality:

This work is original.

2. Author Contributions:

Concept: EÖ,BI; **Conceptualization:** EÖ,SÖ,SK,SRG,BI; **Literature Search:** EÖ,SK,BI; **Data Collection:** EÖ,SÖ; **Data Processing:** EÖ,SÖ; **Analysis:** EÖ,SÖ; **Writing – original draft:** EÖ,BI; **Writing – review & editing:** EÖ,SÖ,SK,SRG,BI.

3. Ethics approval:

This study received approval from the Karamanoğlu Mehmetbey University Medicine Faculty Scientific Ethics Committee (date: 09 December 2025; approval no: 26-2025/23).

4. Funding/Support:

This work has not received any funding or support.

5. Competing Interests:

The authors declare no competing interests.

6. GenAI Usage Statement:

No GenAI tools were used at any stage of the study.

7. Sustainable Development Goals:



REFERENCES

- [1] Galkin, F., Mamoshina, P., Aliper, A., Putin, E., Moskalev, V., Gladyshev, V. N., Zhavoronkov, A. 2020. Human Gut Microbiome Aging Clock Based on Taxonomic Profiling and Deep Learning. *iScience*, 23(6), 101199.
- [2] Guedj, A., Volman, Y., Geiger-Maor, A., Bolik, J., Schumacher, N., Künzel, S., Baines, J. F., Nevo, Y., Elgavish, S., Galun, E., Amsalem, H., Schmidt-Arras, D., Rachmilewitz, J. 2020. Gut microbiota shape 'inflamm-ageing' cytokines and account for age-dependent decline in DNA damage repair. *Gut*, 69(6), 1064-1075.
- [3] Agnoletti, D., Piani, F., Cicero, A. F. G., Borghi, C. 2022. The Gut Microbiota and Vascular Aging: A State-of-the-Art and Systematic Review of the Literature. *Journal of clinical medicine*, 11(12), 3557.
- [4] Behringer E. J. 2023. Impact of aging on vascular ion channels: perspectives and knowledge gaps across major organ systems. *American journal of physiology. Heart and circulatory physiology*, 325(5), H1012-H1038.
- [5] Li, T., Chen, Y., Gua, C., Li, X. 2017. Elevated Circulating Trimethylamine N-Oxide Levels Contribute to Endothelial Dysfunction in Aged Rats through Vascular Inflammation and Oxidative Stress. *Frontiers in physiology*, 8, 350.
- [6] Claesson, M. J., Jeffery, I. B., Conde, S., Power, S. E., O'Connor, E. M., Cusack, S., Harris, H. M., Coakley, M., Lakshminarayanan, B., O'Sullivan, O., Fitzgerald, G. F., Deane, J., O'Connor, M., Harnedy, N., O'Connor, K., O'Mahony, D., van Sinderen, D., Wallace, M., Brennan, L., Stanton, C., ... O'Toole, P. W. 2012. Gut microbiota composition correlates with diet and health in the elderly. *Nature*, 488(7410), 178-184.
- [7] Yatsunenko, T., Rey, F. E., Manary, M. J., Trehan, I., Dominguez-Bello, M. G., Contreras, M., Magris, M., Hidalgo, G., Baldassano, R. N., Anokhin, A. P., Heath, A. C., Warner, B., Reeder, J., Kuczynski, J., Caporaso, J. G., Lozupone, C. A., Lauber, C., Clemente, J. C., Knights, D., Knight, R., ... Gordon, J. I. 2012. Human gut microbiome viewed across age and geography. *Nature*, 486(7402), 222-227.
- [8] Chen, W., Zhang, S., Wu, J., Ye, T., Wang, S., Wang, P., Xing, D. 2020. Butyrate-producing bacteria and the gut-heart axis in atherosclerosis. *Clinica chimica acta; international journal of clinical chemistry*, 507, 236-241.
- [9] Zhang D, Jian YP, Zhang YN, et al. Short-chain fatty acids in diseases. *Cell Commun Signal*. 2023;21(1):212.
- [10] Mariat, D., Firmesse, O., Levenez, F., Guimarães, V., Sokol, H., Doré, J., Corthier, G., Furet, J. P. 2009. The Firmicutes/Bacteroidetes ratio of the human microbiota changes with age. *BMC microbiology*, 9, 123
- [11] Lu, Y., Zhang, Y., Zhao, X., Shang, C., Xiang, M., Li, L., Cui, X. 2022. Microbiota-derived short-chain fatty acids: Implications for cardiovascular and metabolic disease. *Frontiers in cardiovascular medicine*, 9, 900381.
- [12] Wang, Z., Klipfell, E., Bennett, B. J., Koeth, R., Levison, B. S., Dugar, B., Feldstein, A. E., Britt, E. B., Fu, X., Chung, Y. M., Wu, Y., Schauer, P., Smith, J. D., Allayee, H., Tang, W. H., DiDonato, J. A., Lusis, A. J., Hazen, S. L. 2011. Gut flora metabolism of phosphatidylcholine promotes cardiovascular disease. *Nature*, 472(7341), 57-63.
- [13] Sun, X., Jiao, X., Ma, Y., Liu, Y., Zhang, L., He, Y., Chen, Y. 2016. Trimethylamine N-oxide induces inflammation and endothelial dysfunction in human umbilical vein endothelial cells via activating ROS-TXNIP-NLRP3 inflammasome. *Biochemical and biophysical research*

- communications, 481(1-2), 63-70.
- [14] Yao, Y., Xu, Y., Wang, W., Zhang, J., Li, Q. 2017. Glucagon-like peptide-1 improves β -cell dysfunction by suppressing the miR-27a-induced downregulation of ATP-binding cassette transporter A1. *Biomedicine & pharmacotherapy = Biomedecine & pharmacotherapie*, 96, 497-502.
- [15] Alsulami, M., Alamri, H., Barhoumi, T., Munawar, N., Alghanem, B. 2025. The effect of TMAO on aging-associated cardiovascular and metabolic pathways and emerging therapies. *Molecular and cellular biochemistry*, 480(11), 5659-5669.
- [16] Du, Y., Li, X., Su, C., Xi, M., Zhang, X., Jiang, Z., Wang, L., Hong, B. 2020. Butyrate protects against high-fat diet-induced atherosclerosis via up-regulating ABCA1 expression in apolipoprotein E-deficiency mice. *British journal of pharmacology*, 177(8), 1754-1772.
- [17] Fellows, R., Denizot, J., Stellato, C., Cuomo, A., Jain, P., Stoyanova, E., Balázs, S., Hajnády, Z., Liebert, A., Kazakevych, J., Blackburn, H., Corrêa, R. O., Fachi, J. L., Sato, F. T., Ribeiro, W. R., Ferreira, C. M., Perée, H., Spagnuolo, M., Mattiuz, R., Matolcsi, C., ... Varga-Weisz, P. 2018. Microbiota derived short chain fatty acids promote histone crotonylation in the colon through histone deacetylases. *Nature communications*, 9(1), 105.
- [18] Shapiro, H., Thaiss, C. A., Levy, M., Elinav, E. 2014. The cross talk between microbiota and the immune system: metabolites take center stage. *Current opinion in immunology*, 30, 54-62.
- [19] Robles-Vera, I., Toral, M., de la Visitación, N., Aguilera-Sánchez, N., Redondo, J. M., Duarte, J. 2020. Protective Effects of Short-Chain Fatty Acids on Endothelial Dysfunction Induced by Angiotensin II. *Frontiers in physiology*, 11, 277.
- [20] Davie J. R. 2003. Inhibition of histone deacetylase activity by butyrate. *The Journal of nutrition*, 133(7 Suppl), 2485S-2493S.
- [21] Saeedi Saravi, S. S., Pugin, B., Constancias, F., Shabaniyan, K., Spalinger, M., Thomas, A., Le Gludic, S., Shabaniyan, T., Karsai, G., Colucci, M., Menni, C., Attaye, I., Zhang, X., Allemann, M. S., Lee, P., Visconti, A., Falchi, M., Alimonti, A., Ruschitzka, F., Paneni, F., ... Beer, J. H. 2025. Gut microbiota-dependent increase in phenylacetic acid induces endothelial cell senescence during aging. *Nature aging*, 5(6), 1025-1045.
- [22] Zhang, M., Wu, J. F., Chen, W. J., Tang, S. L., Mo, Z. C., Tang, Y. Y., Li, Y., Wang, J. L., Liu, X. Y., Peng, J., Chen, K., He, P. P., Lv, Y. C., Ouyang, X. P., Yao, F., Tang, D. P., Cayabyab, F. S., Zhang, D. W., Zheng, X. L., Tian, G. P., ... Tang, C. K. 2014. MicroRNA-27a/b regulates cellular cholesterol efflux, influx and esterification/hydrolysis in THP-1 macrophages. *Atherosclerosis*, 234(1), 54-64.
- [23] Yue, R., Dutta, A. 2022. Computational systems biology in disease modeling and control, review and perspectives. *NPJ systems biology and applications*, 8(1), 37.
- [24] Pedregosa, F., Varoquaux, G., Gramfort, A., Michel, V., Thirion, B., Grisel, O., Blondel, M., Prettenhofer, P., Weiss, R., Dubourg, V., Vanderplas, J., Passos, A., Duchesnay, É. 2011. Scikit-learn: Machine learning in Python. *the Journal of machine Learning research*, 12, 2825-2830.
- [25] DeGroat, W., Abdelhalim, H., Peker, E., Sheth, N., Narayanan, R., Zeeshan, S., Liang, B. T., Ahmed, Z. 2024. Multimodal AI/ML for discovering novel biomarkers and predicting disease using multi-omics profiles of patients with cardiovascular diseases. *Scientific reports*, 14(1), 26503.
- [26] Barabási, A. L., Oltvai, Z. N. 2004. Network biology: understanding the cell's functional organization. *Nature reviews. Genetics*, 5(2), 101-113.
- [27] Chen, Y., Wang, H., Lu, W., Wu, T., Yuan, W., Zhu, J., Lee, Y. K., Zhao, J., Zhang, H., Chen, W. 2022. Human gut microbiome aging clocks based on taxonomic and functional signatures through

- multi-view learning. *Gut microbes*, 14(1), 2025016.
- [28] Stebegg, M., Silva-Cayetano, A., Innocentin, S., Jenkins, T. P., Cantacessi, C., Gilbert, C., Linterman, M. A. 2019. Heterochronic faecal transplantation boosts gut germinal centres in aged mice. *Nature communications*, 10(1), 2443.
- [29] Ren, J., Li, H., Zeng, G., Pang, B., Wang, Q., Wei, J. 2023. Gut microbiome-mediated mechanisms in aging-related diseases: are probiotics ready for prime time?. *Frontiers in pharmacology*, 14, 1178596.
- [30] Turkish Statistical Institute. Causes of Death Statistics, 2023 - Table 2: Classification by cause of death (ICD-10) Dataset. Ankara: Turkish Statistical Institute. <https://data.tuik.gov.tr/Bulten/Index?p=Olum-ve-Olum-Nedeni-İstatistikleri-2023-53709>. (Access Date, 21.10.2025).
- [31] Efron, B., Tibshirani, R. J. 1994. An introduction to the bootstrap. pp 168-195. New York, NY: Chapman & Hall/CRC, 456p
- [32] Guyon I, Elisseeff, A. 2003. An Introduction to Variable and Feature Selection. *Journal of Machine Learning Research*, 3, 1157-1182.
- [33] Hoyles, L., Fernández-Real, J. M., Federici, M., Serino, M., Abbott, J., Charpentier, J., Heymes, C., Luque, J. L., Anthony, E., Barton, R. H., Chilloux, J., Myridakis, A., Martinez-Gili, L., Moreno-Navarrete, J. M., Benhamed, F., Azalbert, V., Blasco-Baque, V., Puig, J., Xifra, G., Ricart, W., ... Dumas, M. E. 2018. Molecular phenomics and metagenomics of hepatic steatosis in non-diabetic obese women. *Nature medicine*, 24(7), 1070-1080.
- [34] Yang, R., Pang, J., Zhong, X., Pang, S., Hu, X., Wei, C., Yan, W., Chen, X., Zhao, R., Xu, B., Cao, Z. 2025. Molecular mechanisms of aberrant fatty acids metabolism in driving cardiovascular diseases: key regulatory targets and dietary interventions. *Food & function*, 16(15), 5961-5993.
- [35] Budoff, M. J., de Oliveira Otto, M. C., Li, X. S., Lee, Y., Wang, M., Lai, H. T. M., Lemaitre, R. N., Pratt, A., Tang, W. H. W., Psaty, B. M., Siscovick, D. S., Hazen, S. L., Mozaffarian, D. 2025. Trimethylamine-N-oxide (TMAO) and risk of incident cardiovascular events in the multi ethnic study of Atherosclerosis. *Scientific reports*, 15(1), 23362.
- [36] Steyerberg, E. W., Vergouwe, Y. 2014. Towards better clinical prediction models: seven steps for development and an ABCD for validation. *European heart journal*, 35(29), 1925-1931.
- [37] Pencina, M. J., D'Agostino, R. B., Sr, Steyerberg, E. W. 2011. Extensions of net reclassification improvement calculations to measure usefulness of new biomarkers. *Statistics in medicine*, 30(1), 11-21.
- [38] Chen, K., Zheng, X., Feng, M., Li, D., Zhang, H. 2017. Gut Microbiota-Dependent Metabolite Trimethylamine N-Oxide Contributes to Cardiac Dysfunction in Western Diet-Induced Obese Mice. *Frontiers in physiology*, 8, 139.
- [39] Montero-Melendez, T., Dalli, J., Perretti, M. 2013. Gene expression signature-based approach identifies a pro-resolving mechanism of action for histone deacetylase inhibitors. *Cell death and differentiation*, 20(4), 567-575.
- [40] Tang, W. H., Kitai, T., Hazen, S. L. 2017. Gut Microbiota in Cardiovascular Health and Disease. *Circulation research*, 120(7), 1183-1196.
- [41] Canfora, E. E., Meex, R. C. R., Venema, K., Blaak, E. E. 2019. Gut microbial metabolites in obesity, NAFLD and T2DM. *Nature reviews. Endocrinology*, 15(5), 261-273.
- [42] Zhu, W., Gregory, J. C., Org, E., Buffa, J. A., Gupta, N., Wang, Z., Li, L., Fu, X., Wu, Y., Mehrabian, M., Sartor, R. B., McIntyre, T. M., Silverstein, R. L., Tang, W. H. W., DiDonato, J. A., Brown, J. M., Lusi,

- A. J., Hazen, S. L. (2016). Gut Microbial Metabolite TMAO Enhances Platelet Hyperreactivity and Thrombosis Risk. *Cell*, 165(1), 111-124.
- [43] Kurilshikov, A., van den Munckhof, I. C. L., Chen, L., Bonder, M. J., Schraa, K., Rutten, J. H. W., Riksen, N. P., de Graaf, J., Oosting, M., Sanna, S., Joosten, L. A. B., van der Graaf, M., Brand, T., Koonen, D. P. Y., van Faassen, M., LifeLines DEEP Cohort Study, BBMRI Metabolomics Consortium, Slagboom, P. E., Xavier, R. J., Kuipers, F., Hofker, M. H., ... Fu, J. 2019. Gut Microbial Associations to Plasma Metabolites Linked to Cardiovascular Phenotypes and Risk. *Circulation research*, 124(12), 1808-1820.

